

DCCA Enhanced Forced Oscillation Frequency Detection Using Real-world PMU Data

Abraham Canafe*, Yunchuan Liu[†], Lei Yang[†], and Hanif Livani[‡]

* Department of Electrical and Electronics Engineering, California State University, Sacramento, CA 95819

[†] Department of Computer Science and Engineering, University of Nevada, Reno, NV 89557

[‡] Department of Electrical and Biomedical Engineering, University of Nevada, Reno, NV 89557

Abstract—This paper studies forced oscillation frequency detection using real-world Phasor Measurement Unit (PMU) data. The accurate identification of forced oscillations can help operators prevent power system failures and take appropriate remedial actions. To detect forced oscillation frequencies, we first decompose the PMU data into a series of intrinsic mode functions (IMFs) using the Improved Complete Ensemble Empirical Mode Decomposition with Adaptive Noise (ICEEMDAN) technique, which can effectively de-noise the raw PMU data. Then, we choose the optimal mode for frequency detection by selecting the IMF most strongly correlated with the original signal based on detrended cross correlation analysis (DCCA), as real-world PMU data obtained from oscillation events are often non-stationary. Compared with the cross-correlation coefficient used in the existing studies, the DCCA coefficient can better analyze non-stationary data and thus find a better mode for frequency detection. Using the real-world PMU datasets for oscillation events from the ISO-NE grid, experimental results show that the proposed DCCA enhanced forced oscillation frequency detection can accurately detect the oscillation frequency.

Index Terms—PMU, Oscillation Frequency Detection, Improved Complete Ensemble Empirical Mode Decomposition with Adaptive Noise (ICEEMDAN), Detrended Cross-Correlation Analysis (DCCA).

I. INTRODUCTION

The increased deployment of Phasor Measurement Units (PMUs) in power systems has enabled the detection of presence of natural oscillations (NOs) and forced oscillations (FOs) in the power grid. Sustained oscillations can negatively affect the power grid. For example, NOs and FOs can lower the lifespan of equipment, cause power losses, and result in blackouts [1]. Compared to NOs, FOs occur due to external perturbations driving generation sources and can severely affect the safety and reliability of power system operations. Such undesirable effects have motivated the development of various FO detection methods, for a reliable means of detecting forced oscillations enables power grid operators to quickly isolate and remove oscillation sources.

Numerous methods have been proposed for the detection of oscillations using the PMU data, such as Empirical Mode Decomposition (EMD) [2], Variational Mode Decomposition (VMD) [3], Local Mean Decomposition (LMD) [4], Empirical Wavelet Transform (EWT) [5], and Segmented Empirical Wavelet Transform (SEWT) [6], which are shown useful for the detection of sustained oscillations in the power grid.

However, the EMD algorithm and certain EMD variants may face the problem of mode mixing [7] (i.e., multiple frequency components will be contained in the intrinsic mode functions (IMFs)). The problem of mode mixing stems in part from the noisiness of real-world PMU data. To address this challenge, a recent work [1] utilizes Improved Complete Ensemble Empirical Mode Decomposition with Adaptive Noise (ICEEMDAN), which adds a pair of positive and negative noise components to the actual signal to overcome the problem of mode mixing.

Although the FO detection method proposed in [1] is able to decompose PMU data into IMFs more suitable for analysis, the method relies on the standard cross-correlation coefficient for the IMF selection process and thus assumes the presence of a linear relationship [8] between a given IMF and its original signal. Yet, such an assumption may not always hold, as real-world PMU data is often non-stationary [9], a term that characterizes a random process whose statistical properties (such as mean and variance) change over time. Hence, the non-stationary features that may be present in PMU data can lead to the erroneous detection of a FO frequency, which is observed in our case studies in Section III.

To deal with the non-stationarity of PMU data, we propose a FO frequency detection method that leverages the detrended cross-correlation analysis (DCCA) coefficient, which utilizes detrended fluctuation analysis [10] and detrended cross correlation analysis [11]. The use of the DCCA coefficient can improve the IMF selection process described in [1], as it can better characterize the correlation between non-stationary time series [9]. Specifically, we first decompose the PMU data into a series of IMFs using the ICEEMDAN technique, which can effectively de-noise the raw PMU data. Then, we choose the optimal mode for frequency detection by selecting the IMF most strongly correlated with the original signal based on the DCCA coefficient. Compared with the standard cross-correlation techniques used in the existing studies, DCCA can better analyze the non-stationary data and thus find a better mode for frequency detection. Using the real-world PMU datasets for oscillation events from the ISO-NE grid, experimental results show that the proposed DCCA enhanced FO frequency detection can accurately detect the oscillation frequency.

The rest of this paper is structured as follows. Section II introduces the proposed DCCA enhanced FO frequency detection method. Section III presents four case studies of the proposed method using real-world PMU datasets, and Section

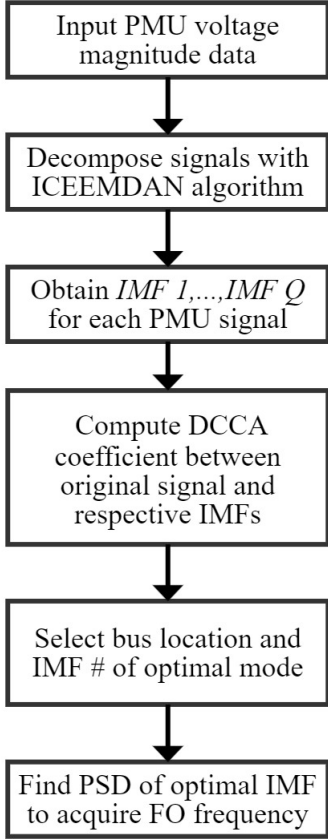


Fig. 1: Workflow of DCCA enhanced FO frequency detection.

IV concludes the paper.

II. DCCA ENHANCED FORCED OSCILLATION FREQUENCY DETECTION

A. Proposed Methodology for FO Frequency Detection Using ICEEMDAN and DCCA

The workflow of the proposed FO frequency detection method is illustrated in Fig. 1. The proposed method first decomposes the input PMU voltage magnitude data into a series of intrinsic mode functions (IMFs) using ICEEMDAN [12] and then chooses the optimal mode for frequency detection by selecting the IMF most strongly correlated with the original signal based on the DCCA coefficient. Similar to [1], the proposed method leverages ICEEMDAN to address the problem of mode mixing [7] (i.e., multiple frequency components will be contained in the IMFs if traditional EMD is used). In contrast with [1], we leverage the DCCA coefficient (instead of the standard cross-correlation coefficient) to select the optimal mode for frequency detection, as the real-world PMU data are non-stationary and the DCCA coefficient can better analyze the non-stationary data (see the case studies using real-world PMU data in Section III).

Specifically, let Y be a $K \times L$ matrix of PMU voltage magnitude measurements, where K denotes the number of

measurements from each PMU and L denotes the number of PMUs. For ease of presentation, we can write Y as

$$Y = [\mathbf{y}_1, \mathbf{y}_2, \dots, \mathbf{y}_L] \quad (1)$$

where \mathbf{y}_l for $l = 1, 2, \dots, L$ denotes a column vector representing the measurements from PMU l .

The proposed method first decomposes each \mathbf{y}_l into a series of IMFs using ICEEMDAN. The set of extracted modes for each \mathbf{y}_l can be denoted by $\{d_{\mathbf{y}_l}^{(q)}\}$, where $q = 1, 2, \dots, Q$. Then, correlation coefficients $\rho_{(d_{\mathbf{y}_l}^{(q)}, \mathbf{y}_l)}$ are computed between each IMF and its associated \mathbf{y}_l using DCCA. The collection of correlation coefficients can be used to build the following $Q \times L$ coefficient matrix,

$$Y_\rho = \begin{bmatrix} \rho_{(d_{\mathbf{y}_1}^{(1)}, \mathbf{y}_1)} & \rho_{(d_{\mathbf{y}_2}^{(1)}, \mathbf{y}_2)} & \cdots & \rho_{(d_{\mathbf{y}_L}^{(1)}, \mathbf{y}_L)} \\ \rho_{(d_{\mathbf{y}_1}^{(2)}, \mathbf{y}_1)} & \rho_{(d_{\mathbf{y}_2}^{(2)}, \mathbf{y}_2)} & \cdots & \rho_{(d_{\mathbf{y}_L}^{(2)}, \mathbf{y}_L)} \\ \vdots & \vdots & \ddots & \vdots \\ \rho_{(d_{\mathbf{y}_1}^{(Q)}, \mathbf{y}_1)} & \rho_{(d_{\mathbf{y}_2}^{(Q)}, \mathbf{y}_2)} & \cdots & \rho_{(d_{\mathbf{y}_L}^{(Q)}, \mathbf{y}_L)} \end{bmatrix}. \quad (2)$$

Using the coefficient matrix Y_ρ , the optimal IMF is selected by choosing the largest coefficient in Y_ρ ,

$$\rho_{(d_{\mathbf{y}_{l^*}}^{(q^*)}, \mathbf{y}_{l^*})} = \max_{q,l} Y_\rho, \quad (3)$$

where q^* and l^* correspond to the q^* -th IMF associated with the l^* -th PMU.

Using the q^* -th IMF associated with the l^* -th PMU, the power spectral density (PSD) of the IMF is computed using Welch's periodogram method [13]. The frequency associated with the highest PSD of the IMF is determined to be frequency of the sustained oscillation.

In the following, we give detailed descriptions of ICEEMDAN and DCCA algorithms used in the proposed FO detection method.

B. ICEEMDAN

The proposed method first decomposes the input PMU voltage magnitude data into a series of IMFs using ICEEMDAN [12]. To de-noise the raw PMU data, controlled noise $\beta_{\mathbf{y}_l}^{(q)} \Gamma_q(w_{\mathbf{y}_l}^{(p)})$ is added to enhance the decomposition of IMFs, where $\Gamma_q(\cdot)$ serves as an operator that uses the EMD algorithm to extract the q -th IMF of its input, and the variable $w_{\mathbf{y}_l}^{(p)}$ denotes the p -th realization of zero-mean, unit-variance Gaussian noise for $p = 1, 2, \dots, P$ (where P is a user-selected constant). The scalar $\beta_{\mathbf{y}_l}^{(q)}$ defined in (4) represents a noise level applied to $\Gamma_q(w_{\mathbf{y}_l}^{(p)})$, i.e.,

$$\beta_{\mathbf{y}_l}^{(q)} = \begin{cases} \epsilon_0 \frac{\text{std}(\mathbf{y}_l)}{\text{std}(\Gamma_1(w_{\mathbf{y}_l}^{(p)}))}, & \text{if } q = 1, \\ \epsilon_0 \text{std}(r_{\mathbf{y}_l}^{(q-1)}), & \text{if } q = 2, 3, \dots, Q \end{cases} \quad (4)$$

In the above equation, ϵ_0 is a user-defined constant, $\text{std}(\cdot)$ represents the standard deviation operator, and $r_{\mathbf{y}_l}^{(q-1)}$ denotes the $(q-1)$ -th residue of the original voltage magnitude signal \mathbf{y}_l .

For each voltage magnitude signal \mathbf{y}_l , a new signal $\mathbf{y}_l^{(p)}$ is first constructed using (5), where $\beta_{\mathbf{y}_l}^{(1)} \Gamma_1(w_{\mathbf{y}_l}^{(p)})$ is added into

\mathbf{y}_l , i.e.,

$$\mathbf{y}_l^{(p)} = \mathbf{y}_l + \beta_{\mathbf{y}_l}^{(1)} \Gamma_1 \left(w_{\mathbf{y}_l}^{(p)} \right). \quad (5)$$

Using (5), we can compute the first residue of the original voltage magnitude signal \mathbf{y}_l , i.e.,

$$r_{\mathbf{y}_l}^{(1)} = \frac{1}{P} \sum_{p=1}^P \Omega \left(\mathbf{y}_l^{(p)} \right), \quad (6)$$

where $\Omega(\cdot)$ returns the local mean of the upper and lower envelopes of $\mathbf{y}_l^{(p)}$, as determined by classical EMD. After the first residue is calculated, (7) can be used to compute the first mode, i.e.,

$$d_{\mathbf{y}_l}^{(1)} = \mathbf{y}_l - r_{\mathbf{y}_l}^{(1)}. \quad (7)$$

Once the first IMF is computed, (8) and (9) can be used to determine the second mode, i.e.,

$$r_{\mathbf{y}_l}^{(2)} = \frac{1}{P} \sum_{p=1}^P \Omega \left(r_{\mathbf{y}_l}^{(1)} + \beta_{\mathbf{y}_l}^{(2)} \Gamma_2 \left(w_{\mathbf{y}_l}^{(p)} \right) \right), \quad (8)$$

$$d_{\mathbf{y}_l}^{(2)} = r_{\mathbf{y}_l}^{(1)} - r_{\mathbf{y}_l}^{(2)}. \quad (9)$$

The remaining residues and modes for $q = 3, \dots, Q$ can then be computed by repeatedly using (10) and (11) until the Q th mode is achieved, i.e.,

$$r_{\mathbf{y}_l}^{(q)} = \frac{1}{P} \sum_{p=1}^P \Omega \left(r_{\mathbf{y}_l}^{(q-1)} + \beta_{\mathbf{y}_l}^{(q)} \Gamma_q \left(w_{\mathbf{y}_l}^{(p)} \right) \right), \quad (10)$$

$$d_{\mathbf{y}_l}^{(q)} = r_{\mathbf{y}_l}^{(q-1)} - r_{\mathbf{y}_l}^{(q)}. \quad (11)$$

C. DCCA Coefficient

Due to the non-stationarity of the signals (see the stationary analysis in Section III), we leverage DCCA to compute the correlation coefficients in (2), which is motivated by the study in [14], showing that DCCA, compared with standard cross-correlation, can better analyze non-stationary data.

To compute the DCCA coefficient between $d_{\mathbf{y}_l}^{(q)}$ and its respective \mathbf{y}_l , we first compute the partial sums $Y_l(k)$ and $D_{\mathbf{y}_l}^{(q)}(k)$ for $k = 1, 2, \dots, K$ using (12) and (13),

$$Y_l(k) = \sum_{k=1}^K (\mathbf{y}_l(k) - \mathbb{E}(\mathbf{y}_l)), \quad (12)$$

$$D_{\mathbf{y}_l}^{(q)}(k) = \sum_{k=1}^K (d_{\mathbf{y}_l}^{(q)}(k) - \mathbb{E}(d_{\mathbf{y}_l}^{(q)})). \quad (13)$$

Starting from $k = 1$, the cumulative sums can then be partitioned into K_n non-overlapping boxes of size n , where $K_n = K/n$ given that K/n is an integer.

For each time window of length n in each integrated series, a polynomial regression is used to compute the local trends $\tilde{Y}_l(k, i)$ and $\tilde{D}_{\mathbf{y}_l}^{(q)}(k, i)$ in each i th non-overlapping closed interval defined on $k \in [(i-1)n+1, ni]$ where $i = 1, \dots, K_n$ [15]. The computed profiles and local trends are then used to create the sample variance functions (14) and (15) and the

sample covariance function (16) i.e.,¹

$$f_{DFA_{\mathbf{y}_l}}(n, i) = \frac{1}{n} \sum_{k=i}^n \left(Y_l((i-1)n+k) - \tilde{Y}_l(k, i) \right)^2, \quad (14)$$

$$f_{DFA_{d_{\mathbf{y}_l}^{(q)}}}(n, i) = \frac{1}{n} \sum_{k=i}^n \left(D_{\mathbf{y}_l}^{(q)}((i-1)n+k) - \tilde{D}_{\mathbf{y}_l}^{(q)}(k, i) \right)^2, \quad (15)$$

$$f_{DCCA_{l,q}}(n, i) = \frac{1}{n} \sum_{k=i}^n \left(Y_l((i-1)n+k) - \tilde{Y}_l(k, i) \right) \times \left(D_{\mathbf{y}_l}^{(q)}((i-1)n+k) - \tilde{D}_{\mathbf{y}_l}^{(q)}(k, i) \right). \quad (16)$$

Averaging the sample variance functions produces the detrended variance functions (17) and (18),

$$F_{DFA_{\mathbf{y}_l}}(n) = \frac{1}{K_n} \sum_{i=1}^{K_n} f_{DFA_{\mathbf{y}_l}}(n, i), \quad (17)$$

$$F_{DFA_{d_{\mathbf{y}_l}^{(q)}}}(n) = \frac{1}{K_n} \sum_{i=1}^{K_n} f_{DFA_{d_{\mathbf{y}_l}^{(q)}}}(n, i). \quad (18)$$

Similarly, the average of the sample covariances (16) yields the detrended covariance function (19),

$$F_{DCCA_{l,q}}(n) = \frac{1}{K_n} \sum_{i=1}^{K_n} f_{DCCA_{l,q}}(n, i). \quad (19)$$

Using (17), (18), and (19), we compute the DCCA coefficient:

$$\rho_{DCCA_{l,q}}(n) = \frac{F_{DCCA_{l,q}}(n)}{\sqrt{F_{DFA_{\mathbf{y}_l}}(n) F_{DFA_{d_{\mathbf{y}_l}^{(q)}}}(n)}}, \quad (20)$$

where $-1 \leq \rho_{DCCA_{l,q}}(n) \leq 1$. As described in [9], $\rho_{DCCA_{l,q}}(n) = 1$ indicates perfect correlation and $\rho_{DCCA_{l,q}}(n) = -1$ indicates perfect anti-cross correlation, whereas a coefficient of $\rho_{DCCA_{l,q}}(n) = 0$ indicates the absence of cross correlation. Thus for the IMF selection procedure described in Section II-A, the IMFs most suitable for analysis in the frequency domain have associated with them DCCA coefficients whose magnitudes $|\rho_{DCCA_{l,q}}(n)|$ are closest to 1.

For each element of Y_ρ , multiple DCCA coefficients can be computed using pre-selected window sizes $n = \alpha_1, \dots, \alpha_\gamma$. The largest absolute value of each set of coefficients is then inserted into the coefficient matrix described in (2):

$$\rho_{(d_{\mathbf{y}_l}^{(q)}, \mathbf{y}_l)} = \max_n |\rho_{DCCA_{l,q}}(n)|. \quad (21)$$

Since the DCCA coefficient is designed to detect cross-

¹If K/n is not an integer, additional non-overlapping boxes that begin at $k = K$ can be created for $Y_l(k)$ and $D_{\mathbf{y}_l}^{(q)}(k)$, and the partial sums used in (14)–(16) can be replaced with $Y_l(K - (i - K_n)n + k)$ and $D_{\mathbf{y}_l}^{(q)}(K - (i - K_n)n + k)$ for $i = K_n + 1, \dots, 2K_n$. For the sake of clarity, this paper treats K as an integer multiple of n , but more details regarding K_n can be found in [14], [16].

correlations from non-stationary data [9] [14], it can be utilized to identify modes that best correlate with a raw, non-stationary PMU voltage magnitude signal. The DCCA coefficient with the largest magnitude indicates the presence of a strong correlation between an IMF and its respective voltage signal.

III. CASE STUDIES

A. Experimental Setup

1) *Datasets*: Historical PMU datasets for oscillation events from the ISO-NE grid (Fig. 2) [17] are used to compare the effectiveness of the cross-correlation and DCCA coefficients for mode selection and FO frequency detection. Voltage magnitude signals are specifically chosen to compare the proposed DCCA-based frequency detection algorithm to the cross correlation-based frequency detection method described in [1]. A brief summary of each oscillation event [17] used in our experiments is provided below:

- *Case 1–June 17, 2016*: The oscillation event occurred in the ISO-NE system on June 17, 2016, originated from a large generator in the Southern part of the Eastern Interconnection and had an oscillation frequency of 0.27 Hz.
- *Case 2–October 3, 2017*: The multi-frequency oscillation event occurred in the ISO-NE system on October 3, 2017. The oscillations came from a generator in Area 3 (Fig. 2) and had dominant mode frequencies of 0.08 Hz, 0.15 Hz, and 0.31 Hz.
- *Case 3–July 20, 2017*: The oscillation event occurred in the ISO-NE system on July 20, 2017. The oscillation originated from a generator in Area 1 (Fig. 2) and had a frequency of 1.13 Hz.
- *Case 4–January 29, 2018*: The oscillation event occurred in the ISO-NE grid on January 29, 2018. The oscillation originated from the generator at substation 7 (Fig. 2) and had an oscillation frequency of 1.57 Hz.

2) *Implementation*: As a preprocessing procedure, missing values from the PMU datasets for each case were dropped, and linear interpolation was applied to replace missing PMU data. It should be noted that no bandpass filters were used. The DCCA-based frequency detection method proposed in this paper and the frequency detection method described in [1] were then applied to each set of PMU voltage magnitude signals. A matrix of PMU measurements was constructed using (1), and after the ICEEMDAN algorithm was applied to each voltage magnitude signal, coefficient matrices for the cross-correlation coefficient and the DCCA coefficient were created using (2). Since the ICEEMDAN algorithm extracted varying numbers of IMFs from each \mathbf{y}_l , NaN values were added to ensure that each Y_ρ was an $Q \times L$ rectangular matrix. Once the optimal IMFs were selected using (3), the power spectral density of the decomposed signal was computed using a 50% overlap, and the FO frequencies associated with the cross-correlation and DCCA coefficients were estimated.

The PyEMD Python package was used to carry out the ICEEMDAN algorithm [18]. In this paper, $P = 20$ realizations were produced during the computation of each IMF, and a scaling factor of $\epsilon_0 = 0.005$ was used. Similarly, the

TABLE I: Stationary analysis of ISO-NE PMU time series selected by the cross-correlation and DCCA coefficients.

Case #	Cross-correlation	DCCA
1	Stationary	Stationary
2	Non-stationary	Non-stationary
3	Non-stationary	Non-stationary
4	Non-stationary	Non-stationary

TABLE II: Frequency detection results of ISO-NE oscillation events using cross-correlation (Xcorr) and DCCA.

Case #	Coefficient	Bus Location	IMF #	ρ	$f_{detected}$	f_{actual}
1	Xcorr	Sub:1:Ln:1.1	4	0.910	0.264 Hz	0.27 Hz
	DCCA	Sub:9:Ln:21.1	4	0.984	0.264 Hz	
2	Xcorr	Sub:1:Ln:1.1	10	0.661	0.0293 Hz	0.31 Hz
	DCCA	Sub:1:Ln:1.1	4	0.894	0.352 Hz	
3	Xcorr	Sub:6:Gen:Gen1.1	2	0.880	1.143 Hz	1.13 Hz
	DCCA	Sub:2:Ln:4.1	1	0.986	1.143 Hz	
4	Xcorr	Sub:3:Ln:6.1	10	0.781	0.0293 Hz	1.57 Hz
	DCCA	Sub:7:Ln:15.1	3	0.851	1.582 Hz	

fathom Python package [16] was used to create the coefficient matrix of DCCA coefficients (2). Each $\rho_{(d_{y_l}^{(q)}, y_l)}$ was calculated using first-order polynomial regressions with window sizes $n = 20, 21, \dots, 100$.

B. Stationarity Analysis

We analyze the stationarity of PMU signals during oscillation events. Specifically, we leverage the Augmented Dickey Fuller (ADF) test [19] and the Kwiatkowski-Phillips-Schmidt-Shin (KPSS) test [20] to analyze the stationarity of the raw voltage magnitude signals that are selected based on the cross-correlation and DCCA coefficients. From Table I, we observe that the signals selected based on the cross-correlation and DCCA coefficients are not stationary in all the cases except Case 1. Since it has been demonstrated that the DCCA coefficient can perform well when used for the analysis of non-stationary time series [14], it is reasonable to expect that the DCCA coefficient would outperform the cross-correlation coefficient in terms of selecting an IMF characterized by a dominant FO frequency. This is confirmed by the experimental results in the next section.

C. Frequency Detection: Cross-correlation v.s. DCCA

Table II shows the FO frequencies detected using the cross-correlation and DCCA coefficients under different cases. It can be observed that the cross-correlation based frequency detection can perform well for stationary signals (Case 1), but may fail for non-stationary signals (Case 2 and Case 4), whereas the proposed DCCA based frequency detection method can accurately detect a dominant FO frequency from both stationary and non-stationary signals.

Due to the non-stationarity of PMU data in Case 2 and Case 4, using the standard cross-correlation coefficient may not find the best IMF for frequency detection:

- In Case 2, the standard cross-correlation coefficient selects an IMF clearly unsuitable for analysis (Fig. 3), whereas the DCCA coefficient selects an IMF whose oscillation frequency more closely resembles the actual oscillation frequency of 0.31 Hz (Fig. 4). The power spectral density of the IMF selected by the cross-correlation

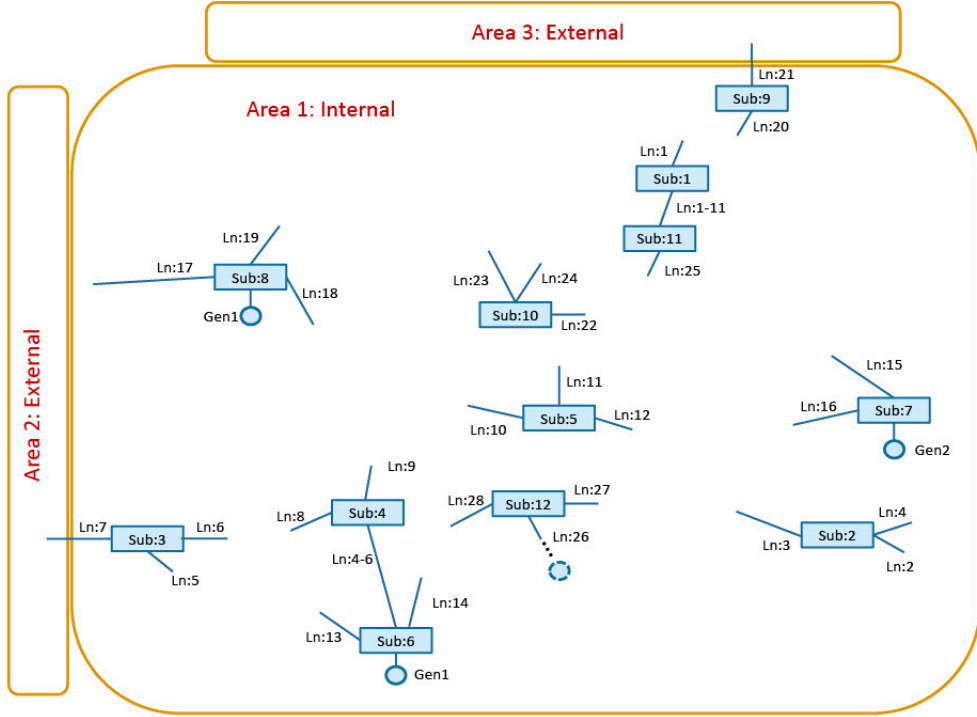


Fig. 2: Topology for ISO-NE system [17].

coefficient, depicted in Fig. 3(c), fails to preserve the expected FO frequency. On the other hand, the power spectral density generated from the optimal mode selected by the DCCA coefficient, shown in Fig. 4(c), returns a distribution that retains the FO frequency component.

- In Case 4, the DCCA coefficient indisputably outperforms the cross-correlation coefficient, for IMF 7, which is extracted from substation 7 (Fig. 2), yields a dominant mode frequency close in approximation to the expected frequency of 1.57 Hz. The mode selected by the DCCA coefficient for Case 4 contains frequency components intuitively usable for analysis (Fig. 6), an observation evidenced by the maximum power spectral density of 1.582 Hz shown in Fig. 6(c). However, the cross-correlation coefficient selects an IMF that does not keep the frequency components of its original voltage magnitude signal, as shown by the power spectral density of the IMF depicted in Fig. 5(c).

Since the stationarity tests from Table I show that the cross-correlation and DCCA coefficients attempt to select optimal IMFs from raw, non-stationary voltage magnitude data for the Case 2 and Case 4 datasets, it can be observed that the DCCA coefficient demonstrates an ability to detect correct FO frequencies from non-stationary PMU data, a capability that the standard cross-correlation coefficient fails to show.

IV. CONCLUSIONS

In this paper, we propose a FO frequency detection method that leverages the detrended cross-correlation analysis (DCCA)

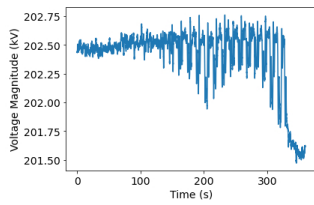
coefficient, which utilizes detrended fluctuation analysis and detrended cross correlation analysis. The use of the DCCA coefficient can improve the IMF selection process by better characterizing the correlation between non-stationary time series. Specifically, we first decompose the PMU data into a series of IMFs using the ICEEMDAN technique, which can effectively de-noise the raw PMU data. Then, we choose the optimal mode for frequency detection by selecting the IMF most strongly correlated with the original signal based on DCCA. Compared with the standard cross-correlation coefficient used in the existing studies, the DCCA coefficient can better analyze the non-stationary data and thus find a better mode for frequency detection. Using real-world PMU datasets for oscillation events from the ISO-NE grid, experimental results show that the proposed DCCA enhanced FO frequency detection can accurately detect the oscillation frequency.

V. ACKNOWLEDGEMENTS

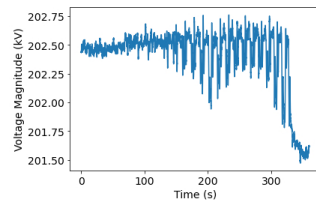
This work is supported by the National Science Foundation Grant CNS-1950485.

REFERENCES

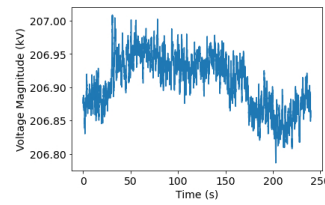
- [1] M. Zuhaib, M. Rihan, and M. T. Saeed, "A novel method for locating the source of sustained oscillation in power system using synchrophasors data," *Protection and Control of Modern Power Systems*, vol. 5, no. 1, pp. 1–12, 2020.
- [2] N. E. Huang, Z. Shen, S. R. Long, M. C. Wu, H. H. Shih, Q. Zheng, N.-C. Yen, C. C. Tung, and H. H. Liu, "The empirical mode decomposition and the hilbert spectrum for nonlinear and non-stationary time series analysis," *Proceedings of the Royal Society of London. Series A: mathematical, physical and engineering sciences*, vol. 454, no. 1971, pp. 903–995, 1998.



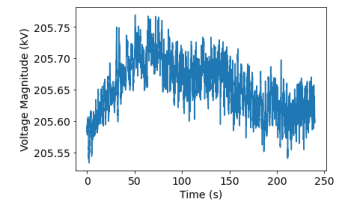
(a) Voltage magnitude signal (substation 1) selected using cross-correlation.



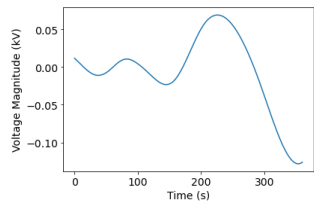
(a) Voltage magnitude signal (substation 1) selected using DCCA.



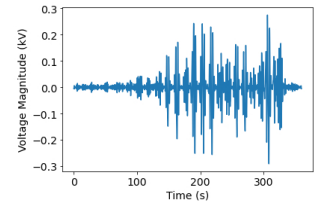
(a) Voltage magnitude signal (substation 3) selected using cross-correlation.



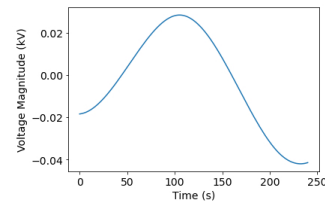
(a) Voltage magnitude signal (substation 7) selected using DCCA.



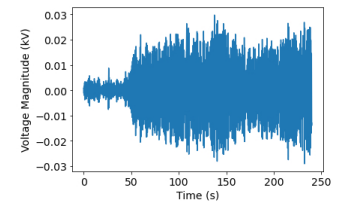
(b) Optimal mode (IMF 10) selected using cross-correlation.



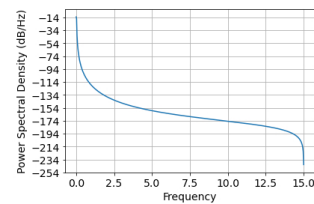
(b) Optimal mode (IMF 4) selected using DCCA.



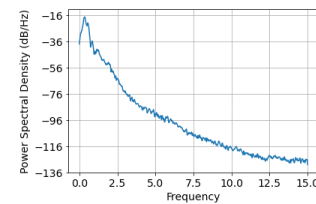
(b) Optimal mode (IMF 10) selected using cross-correlation.



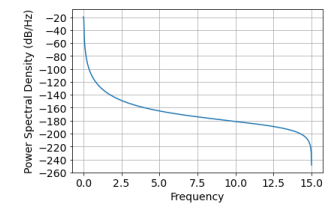
(b) Optimal mode (IMF 3) selected using DCCA.



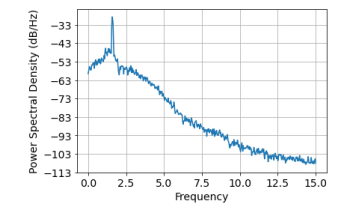
(c) Power spectral density of IMF 10.



(c) Power spectral density of IMF 4.



(c) Power spectral density of IMF 10.



(c) Power spectral density of IMF 3.

Fig. 3: Frequency detection using cross-correlation coefficient for Case 2.

Fig. 4: Frequency detection using the DCCA coefficient for Case 2.

Fig. 5: Frequency detection using the cross-correlation coefficient for Case 4.

Fig. 6: Frequency detection using the DCCA coefficient for Case 4.

- [3] K. Dragomiretskiy and D. Zosso, "Variational mode decomposition," *IEEE Transactions on Signal Processing*, vol. 62, no. 3, pp. 531–544, 2014.
- [4] J. S. Smith, "The local mean decomposition and its application to eeg perception data," *Journal of the Royal Society Interface*, vol. 2, no. 5, pp. 443–454, 2005.
- [5] J. Gilles, "Empirical wavelet transform," *IEEE Transactions on Signal Processing*, vol. 61, no. 16, pp. 3999–4010, 2013.
- [6] A. Khurram, A. Gusnanto, and P. Aristidou, "Detection of oscillatory modes in power systems using empirical wavelet transform," in *2021 IEEE Madrid PowerTech*, pp. 1–6, 2021.
- [7] H.-P. Huang, S.-Y. Wei, H.-H. Chao, C. F. Hsu, L. Hsu, and S. Chi, "An investigation study on mode mixing separation in empirical mode decomposition," *IEEE Access*, vol. 7, pp. 100684–100691, 2019.
- [8] A. F. Kohn, "Autocorrelation and cross-correlation methods," *Wiley Encyclopedia of Biomedical Engineering*, 2006.
- [9] G. Zebende, "Dcca cross-correlation coefficient: Quantifying level of cross-correlation," *Physica A: Statistical Mechanics and its Applications*, vol. 390, no. 4, pp. 614–618, 2011.
- [10] C.-K. Peng, S. V. Buldyrev, S. Havlin, M. Simons, H. E. Stanley, and A. L. Goldberger, "Mosaic organization of dna nucleotides," *Phys. Rev. E*, vol. 49, pp. 1685–1689, Feb 1994.
- [11] B. Podobnik and H. E. Stanley, "Detrended cross-correlation analysis: A new method for analyzing two nonstationary time series," *Phys. Rev. Lett.*, vol. 100, p. 084102, Feb 2008.
- [12] M. A. Colominas, G. Schlotthauer, and M. E. Torres, "Improved complete ensemble emd: A suitable tool for biomedical signal processing," *Biomedical Signal Processing and Control*, vol. 14, pp. 19–29, 2014.
- [13] P. Welch, "The use of fast fourier transform for the estimation of power spectra: A method based on time averaging over short, modified periodograms," *IEEE Transactions on Audio and Electroacoustics*, vol. 15, no. 2, pp. 70–73, 1967.
- [14] L. Kristoufek, "Measuring correlations between non-stationary series with dcca coefficient," *Physica A: Statistical Mechanics and its Applications*, vol. 402, pp. 291–298, 2014.
- [15] C. Bachechi, F. Rollo, and L. Po, "Detection and classification of sensor anomalies for simulating urban traffic scenarios," *Cluster Computing*, Nov 2021.
- [16] S. Bianchi, "fathon: A python package for a fast computation of detrended fluctuation analysis and related algorithms," *Journal of Open Source Software*, vol. 5, no. 45, p. 1828, 2020.
- [17] S. Maslennikov, B. Wang, Q. Zhang, a. Ma, a. Luo, a. Sun, and E. Litvinov, "A test cases library for methods locating the sources of sustained oscillations," in *2016 IEEE Power and Energy Society General Meeting (PESGM)*, pp. 1–5, 2016.
- [18] D. Laszuk, "Python implementation of empirical mode decomposition algorithm." <https://github.com/laszukdawid/PyEMD>, 2017.
- [19] D. A. Dickey and W. A. Fuller, "Distribution of the estimators for autoregressive time series with a unit root," *Journal of the American Statistical Association*, vol. 74, no. 366, pp. 427–431, 1979.
- [20] D. Kwiatkowski, P. C. Phillips, P. Schmidt, and Y. Shin, "Testing the null hypothesis of stationarity against the alternative of a unit root: How sure are we that economic time series have a unit root?," *Journal of Econometrics*, vol. 54, no. 1, pp. 159–178, 1992.